SYNTHESIS AND CHARACTERIZATION OF PROMISING CATHODE MATERIALS ($LiNi_XMn_{2-X}O_4$) FOR LITHIUM ION BATTERY

BY

BOKA FIKADU

A THESIS SUBMITTED TO THE DEPARTMENT OF APPLIED PHYSICS PROGRAM

SCHOOL OF APPLIED NATURAL SCIENCES

PRESENTED IN PARTIAL FULFILLMENT OF THE REQUIREMENTS FOR THE DEGREE OF MASTER'S OF SCIENCE IN APPLIED PHYSICS (LASER SPECTROSCOPY)

OFFICE OF GRADUATE STUDIES

ADAMA SCIENCE AND TECHNOLOGY UNIVERSITY

ADAMA, ETHIOPIA

JUNE, 2019

SYNTHESIS AND CHARACTERIZATION OF PROMISING CATHODE MATERIALS ($LiNi_XMn_{2-X}O_4$) FOR LITHIUM ION BATTERY

By

Boka Fikadu Banti

Advisor: Leta Tesfaye (PhD)

Co-Advisor: Alemu Kebede (PhD)

A Thesis Submitted To The Department Of Applied Physics Program

School Of Applied Natural Sciences

Presented In Partial Fulfillment Of The Requirements For The Degree Of Master's Of Science

In Applied Physics (Laser Spectroscopy)

Office Of Graduate Studies

Adama Science And Technology University

Adama, Ethiopia

June, 2019

ADAMA SCIENCE AND TECHNOLOGY UNIVERSITY

POSTGRADUATE PROGRAM

SCHOOL OF APPLIED NATURAL SCIENCE

APPLIED PHYSICS PROGRAM

As thesis research advisor, I hereby certify that I have read and evaluated this thesis entitled: "**Synthesis and characterization of promising cathode materials ($LiNi_xMn_{2-x}O_4$) for lithium ion battery**" prepared under my guidance by **Boka Fikadu**. I recommend that it can be submitted as fulfilling the thesis requirement.

Boka Fikadu	_____	_____
Student	Signature	Date
Dr. Leta Tesfaye	_____	_____
Advisor	Signature	Date
Dr. Alemu Kebede	_____	_____
Co-Advisor	Signature	Date

As members of the Board of Examiners of the M.Sc. thesis Open Defense Examination, we certify that we have read and evaluated the thesis work prepared by **Boka Fikadu** and examined the candidate. We recommended that the thesis be accepted as fulfilling the thesis requirement for the Degree of Master of Science in Physics.

_____	_____	_____
Chairperson	Signature	Date
_____	_____	_____
Internal Examiner	Signature	Date
_____	_____	_____
External Examiner	Signature	Date

Declaration and Statement of the Candidate

I solemnly declare that this thesis work is not submitted to any other institution anywhere for the award of any academic degree, diploma, or certificate. Brief quotations from this thesis are allowable without special permission provided that accurate acknowledgement of source is made. Requests for permission for extended quotation from or reproduction of this manuscript in whole or in part may be granted by the head of department or the Dean of the School of Graduate Studies when in his or her judgment the proposed use of the material is in the interests of scholarship. In all other instances, however, permission must be obtained from the author.

Name of candidate: Boka Fikadu Signature: _____

Place: Adama Science and Technology University, Adama

Date of Submission: June 2019

Acknowledgements

First of all, I would like to thank almighty God who gave me the chance to successfully accomplished my study. Next, I would like to thank my advisor: Dr. Leta Tesfaye and Co-advisor: Dr. Alemu Kebede for their constructive comments, guidance and endless support from the beginning to the end throughout my study. I am also grateful for their insightful lectures that I took advantage of writing this thesis. I respectfully thank ASTU and Department of Applied Physics Program for giving me the sponsorship to study my M.Sc. Finally, I would like to express thanks from bottom of my heart, to all my family members and my entire instructor at ASTU. My special thanks goes to, my wife, Hana Bedasa, for her love, and continuous support. Last but not least, my heartfelt gratitude goes to fellow friends and colleagues. They deserve special thanks for their valuable contributions and encouragement.

Table of contents

Contents **Page**

List of Tables

List of Figures

List of Symbols and Achromies

Li	Lithium
Al	Aluminium
Ni	Nickel
LMO	Lithium manganese oxide
Li ion	Lithium ion
LIBs	Lithium ion batteries
EVs	Green energy vehicles
O	Oxidizing
XRD	X-ray diffraction
R	Reducing
θ	Theta
N	Nitrogen
H	Hydrogen
O	Oxygen
C	Carbon
SEM	Scanning electron microscopy
SCM	Solution combustion method
Re	Equivalent ratio
M	molecular weight
T	Temperature(k)
P	number of Mn(III)
C_T	Theoretical capacity (mAh/g)

Abstract

In this study, we have synthesized $LiNi_xMn_{2-x}O_4$ (x=0, 0.125, 0.25, 0.375, and 0.5) cathode materials for Li-ion battery using metal nitrates and urea as precursors by solution combustion method. The samples were characterized by scanning electron microscopy (SEM), Thermo-gravimetric Analysis (TGA), and X-Ray diffraction (XRD) results. X-Ray diffraction characterization demonstrated that a basic crystallized spinel phase was already formed in the primary product from the direct combustion process, while pure phase $LiMn_2O_4$ was obtained after further calcination in air at relatively low temperature of 600 °C. The scanning electro-microscopy (SEM) analyzed the spinels revealed essentially spherical morphology. The Thermo-Gravimetric Analysis (TGA) showed that the mass loss curve exhibited a continuous decrease of mass with temperature. The electrochemical performance of all the cathode samples prepared using the solution combustion method is comparable to those reported for Nickel-doped $LiMn_2O_4$ spinel cathode materials. As a result, the as-prepared $LiMn_2O_4$ showed a favorable capacity of 114 mAh/g at a current rate of 0.2C and still retained a capacity of 84 mAh/g at 5 C. After 100 continuous cycles at 0.1C, a capacity of 108 mAh/g was still maintained, compared to 120 mAh/g at the first cycle. The results demonstrated that combustion synthesis-derive $LiMn_2O_4$ is a promising cathode material for lithium ion batteries (LIBs).

Keywords: Solution combustion method, Ni doped $LiMn_2O_4$, experimental, COMSOL Multiphysics, Li ion battery

Chapter 1: Introduction

1.1 Background of the Study

A battery is a device that converts chemical energy, which is stored inside of its electrodes, into electric power by means of electrochemical redox reactions. Among the various types of batteries, Lithium-ion battery (LIB) is one of the most popular types of rechargeable battery for portable electronics and power tool equipments, with the best energy densities and a slow loss of charge when not in use [1 – 3]. A conventional battery must have three main components: cathode, electrolyte and anode. During these decades rechargeable lithium ion batteries have been studied and widely applied in all different kinds of electronic products such as notebooks, mobile phones and portable electronic devices. Nowadays, they have been increasingly used in electric vehicles (EV) and hybrid electric vehicles (HEV) because of their high power density, long cycle life and no memory effect are used in practical lithium ion batteries on the market.

$LiMn_2O_4$ (LMO) spinel being one of the most promising positive (cathode) materials attracted the interest of researchers, due to its low cost, environmental friendliness and good safety [4,5]. However, the problem with spinel $LiMn_2O_4$ cathode material is it suffers severe capacity loss upon repeated charge-discharge cycling at elevated temperature. Some of the causes for capacity fading might be related with Mn dissolution in acidic electrolytes via the disproportionate reaction: $2Mn^{3+} \rightarrow Mn^{2+} + Mn^{4+}$ [6] Jahn-Teller distortion of Mn^{3+} at deeply discharge state [4], and oxygen deficiency [7]. In order to tackle this problem, several research groups have synthesized cation substituted spinel materials $LiM_xMn_{2-x}O_4$ such as (M= Ni, Al, Fe, Co) with an intention of getting high-potential plateaus as well as increasing the cyclability. The compound $LiNi_{0.5}Mn_{1.5}O_4$ with a cubic spinel structure has been characterized as a high potential around 4.9 V cathode materials for lithium ion batteries [8]. However, the high amount of nickel in this spinel makes it more expensive than the LMO. Thus, it is very crucial to strategically improve the electrochemical performance of LMO by substituting it with a very low amount of nickel. In this work, we showed that substituting

the LMO with low nickel concentration greatly increase the energy storage, capacity retention or cyclability, and lithium ion diffusion ability of the spinel.

Lithium ion batteries are increasingly used. The improvement of the energetic density allows a bigger autonomy for a lower weight. Lithium batteries are even used in aviation with the Efan (Fully powered by electricity airplane). The performance and life of a battery pack is related to its temperature. To have a maximum efficiency the temperature of the pack must be within a specific range. The numerical simulation with thermal effects is a good way to develop and improve battery packs at lower cost than experimentation.

The electrochemical performance of cathode materials varies with the synthesis methods. Generally, $LiNi_xMn_{2-x}O_4$ cathode materials were synthesized by conventional solid-state method [10,11]. However, this method needs mixing of lithium sources with manganese source mechanically and followed by high temperature reaction which usually takes many hours. Besides, the solid-state reaction $LiNi_xMn_{2-x}O_4$ spinel materials will have impurity and poor Control of stoichiometry. Homogeneous dispersion of the cation substituting element in crystal lattice is so crucial in the synthesis of substituted $LiM_xMn_{2-x}O_4$ (M = substituting cation) cathode materials. Unlike solid-state reaction, solution synthesis techniques are more preferable to obtain homogeneous composition with minimal or no impurity. Several solution synthesis methods of cation-substituted $LiMn_2O_4$ spinel structure have been reported, such as a spray-drying method [12], emulsion-drying method [13]molten salt method [14], sol-gel method [15]. However, most of these methods involve complicated treatment processes or expensive reagents, which are time consuming and high cost for commercial applications. Solution-combustion method (SCM) has emerged as one of the most preferred wet synthetic methods.

In our present work, we synthesize spherically-shaped spinel $LiNi_xMn_{2-x}O_4$ (x =0, 0.125, 0.25, 0.375 and 0.5) cathode materials with superior capacity retention following one-step time efficient and cheap SCM. It should be noted that spherically-shaped cathode materials with homogeneously distributed microsize particles are preferred to get a better capacity performance from spinel cathode materials [16, 17].

1.2 Statement of the problem

The recent accidents of fires in Li-ion battery packs upon crushed by metal objects in the promising Tesla Model S cars highlights the importance of battery safety. Therefore, active research is continuing in all aspects of batteries, from anode, cathode, separator, electrolyte, safety, thermal control, packaging, to cell construction and battery management.

There have been several studies of synthesizing cathode materials ($LiNi_xMn_{2-x}O_4$) for lithium ion battery by using solution combustion to increase energy storage and capacity retention, there is no considered due to COMSOL Multiphysics. In this work, based on COMSOL Multiphysics and with experimental of solution combustion to synthesis of promising cathode materials ($LiNi_xMn_{2-x}O_4$) for lithium ion battery. Then, the study of this proposal of the project is to investigate the synthesis and characterization of promising cathode materials ($LiNi_xMn_{2-x}O_4$) for lithium ion battery by substituting some cation atom using solution combustion and COMSOL Multiphysics inorder to increase energy storage and capacity retention.

1.3 Objectives of the study

The main objective of this study is to synthesis and characterization of promising cathode materials ($LiNi_xMn_{2-x}O_4$) for lithium ion battery using solution combustion in order to increase energy storage and capacity retention.

The specific objectives of the study are:

- To synthesis promising cathode materials ($LiNi_xMn_{2-x}O_4$) for lithium ion battery using doping some amount of cation atom.
- To characterize promising cathode materials ($LiNi_xMn_{2-x}O_4$) for lithium ion battery using SEM, XRD, and TGA.

1.4 Thesis Outlines

This thesis organized into five chapters. **Chapter two** includes review of related literatures. It contains nine sections. It deals with the theory of Lithium ion battery, Cathode materials with their types, Anode, Electrolytes, separators, Mechanisms of lithium ion battery, Progress in lithium ion battery and COMSOL Multiphysics. **Chapter three** presents the

overall materials and methods by which important data is collected and analyzed. **Chapter four** covers the results and discussion of the study. **Chapter five** gives the conclusions of entire parts of this work and describes the results obtained in chapter 4.

Chapter 2: Literature Review

2.1 Lithium -Ion Battery

A lithium-ion battery is an advanced battery technology that uses lithium ions as a key component of its electrochemistry. An electrical battery is one or more electrochemical cells that convert stored chemical energy into electrical energy. There are two major types of batteries: These are primary and secondary batteries. Primary batteries are those which cannot be recharged because the chemical reaction inside the battery cannot be reversed and once used it must be discarded. Secondary batteries can be recharged and can be reused multiple times. A Li-ion battery usually refers to a secondary battery in which energy is stored chemically through redox reactions that employ lithium intercalation between the positive (cathode) and the negative (anode) electrodes. They are currently the dominant mobile power sources for portable electronic devices, exclusively used in cell phones and laptop computers [19].

Li-ion batteries are considered the powerhouse for the personal digital electronic revolution starting from about two decades ago, roughly at the same time when Li-ion batteries were commercialized. As one may has already noticed from his/her daily life, the increasing functionality of mobile electronics always demand for better Li-ion batteries. For example, to charge the cell phone with increasing functionalities less frequently as the current phone will improve quality of one's life. Another important expanding market for Li-ion batteries is electric and hybrid vehicles, which require next-generation Li-ion batteries with not only high power, high capacity, high charging rate, long life, but also dramatically improved safety performance and low cost. Figure 1 is a schematic of a lithium-ion battery. The main components are the current collectors, the electrodes, the anode and cathode and the separator. The electrodes are made up of active storage particles, binder and filler. Electrolyte fills the pores of the structure, including both electrodes and the separator. Lithium-ions flow through the separator from the anode to the cathode during discharge and vice-versa during the charging process.

For the cathode in current technology, these particles consist of materials that are layered at the atomic scale, typically Oxides, such as lithium manganate and lithium cobalt oxide. For the anode the conventional material in use today is graphite. In both electrodes, the lithium is stored in the space between the atomic layers, usually in the form of its Li^+ ion with an electron localized adjacent to it in the atomic structure, a feature required by electrical neutrality. The electrodes are porous structures with storage particles embedded in a polymeric binder, e.g. polyvinylidene fluoride (PVDF), with the porosity designed to give the electrolyte access to the storage particles. In some cases, carbon black particles are added to the cathode to boost the electronic conductivity, while in others carbon black is coated on the storage particles. The entire battery, including both electrodes and the separator, is filled with the electrolyte. In current technology, this normally consists of a lithium-based ionic salt, e.g. $LiPF_6$, dissolved in an organic liquid solvent.

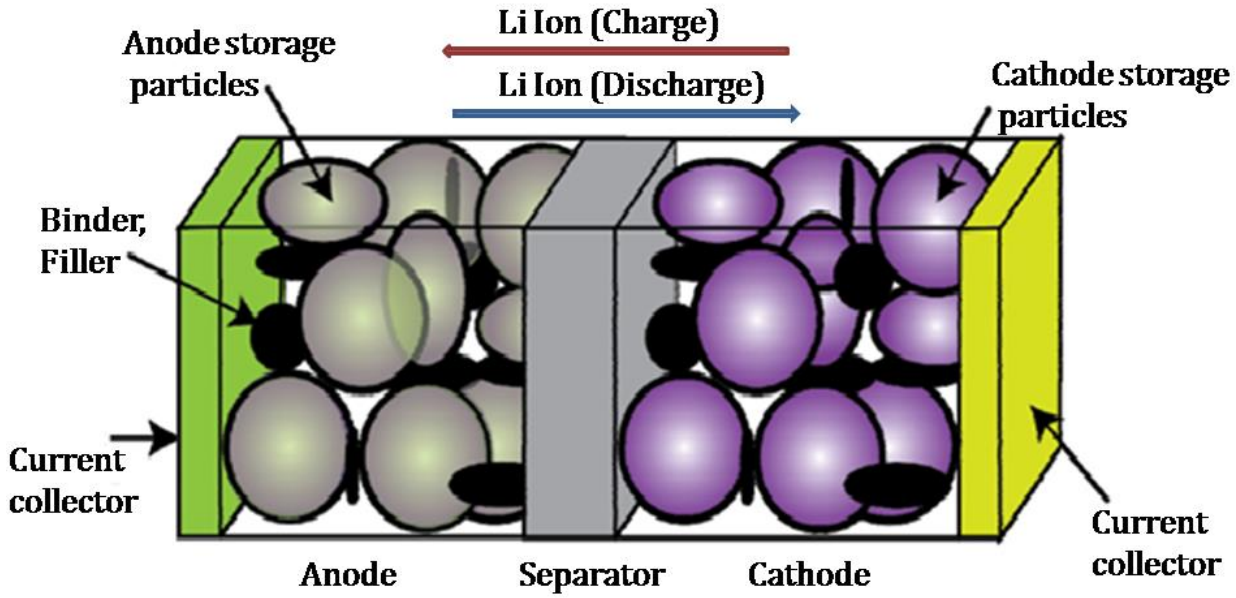

Figure 1. A schematic of the structure of the lithium ion battery [19].

During the discharge process, i.e. the use of the battery to supply electrical energy, lithium stored in the anode at the storage particle surface is oxidized to its ionic form by removal of the localized electron, is extracted from the particle and replaced by further lithium atoms that diffuse from the interior of the particles. The resulting Li^+ ions move through the electrolyte to the separator and thence to the storage particles in the cathode, whereas the

electrons cannot pass through the separator. As a consequence, the electrons flow through the graphite particles to the anode current collector and then to an external circuit connected to the cathode current collector. From there, the electrons are transported through the carbon black in the cathode to the surface of the cathode storage particles, where they recombine with lithium ions.

The lithium is then inserted into the storage particles; through which it diffuses by solid state transport until a uniform concentration is reached. During the battery charging process the reverse occurs, with lithium leaving storage particles in the cathode and moving into storage particles in the anode, while electrons are driven round the external electrical circuit by the charging device. The process of inserting lithium ions into the storage particles is known as intercalation. This can be defined formally as the insertion of a guest species into normally unoccupied interstitial sites in the crystal structure of an existing stable host material [20]. Though the chemical composition of the host phase initially present can be substantially modified, the basic crystal structure is preserved. The addition of an interstitial species causes a change in volume: this leads to strain, and, when it is heterogeneous, this causes mechanical stress.

A Li-ion battery usually refers to a secondary battery in which energy is stored chemically through redox reactions that employ lithium intercalation between the positive (cathode) and the negative (anode) electrodes i.e. as a battery is charged and discharged the lithium ions move back and forth between the cathode and the anode because of this they are also referred as “Rocking-chair” batteries [21]. Basically there are four primary components of a lithium-ion battery: the anode, cathode, separator and electrolyte for which a variety of materials may be used. The cathode acts as a positive electrode which accepts the electrons while reducing and the anode acts as a negative electrode which donates the electrons and oxidizes during the discharge cycles. The electrodes do not touch each other but are electrically connected by the electrolyte while the separator prevents the mixing between them but allows ions to flow.

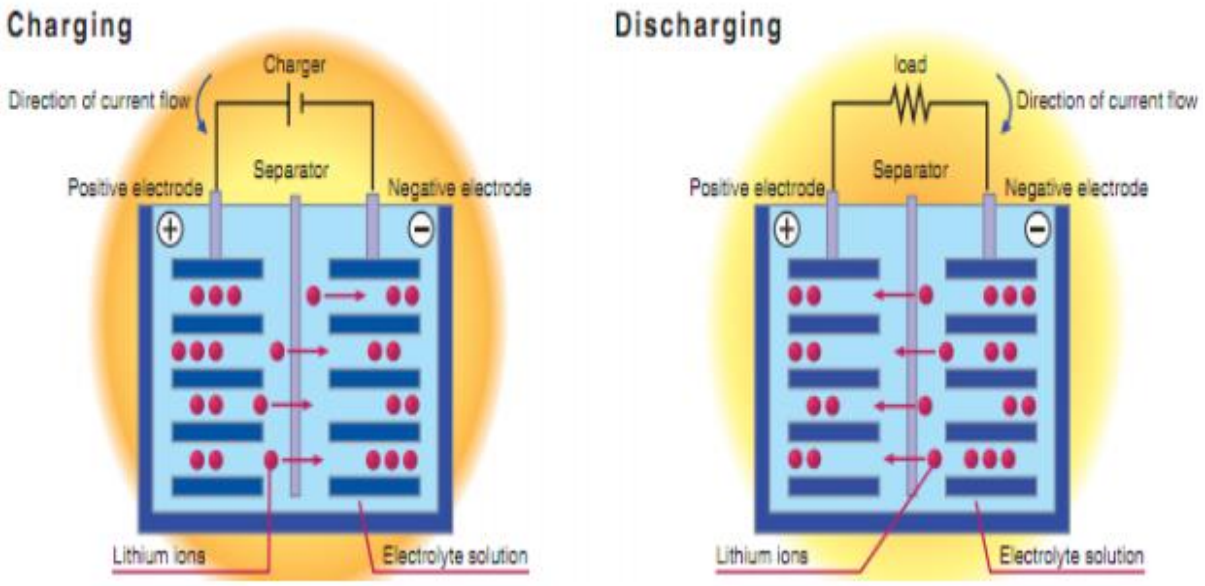

Figure 2: Diagram of Li-ion cell during charging and discharging **[22]**.

To understand this process briefly we can consider the example of a standard $LiCoO_2$ battery in which $LiCoO_2$ acts as a cathode. During charging, lithium ions move from cathode to anode and electrons are removed from cathode by an external field and then are transferred to anode. During discharge, anode supplies the ions to electrolyte and electrons to the external circuit where the ions intercalate into cathode and electrons from the external circuit for charge compensation.

2.2 Cathode Materials

There are a number of candidates that have been explored as cathode materials for Li-ion batteries. The cathode materials can be categorized based on voltage versus lithium. Typically: 2-Volt cathode materials are TiS_2 and MoS_2 with 2-D layered structure; 3-Volt cathode materials are MnO_2 and V_2O_5; 4-Volt cathode materials are $LiCoO_2$, $LiNiO_2$ with 2-D layered structure and 3-D spinel $LiMn_2O_4$ and olivine $LiFePO_4$; 5-Volt cathode materials are olivine $LiMnPO_4$, $LiCoPO_4$, and $Li_2M_xMn_{4-x}O_8$ (M = Fe, Co) spinel 3-D structure. Generally, high cathode voltage is desirable as energy stored is proportional to the cell operating voltage. However, electrolyte stability has to be taken into consideration in selecting high voltage cathode materials.

Cathode materials for lithium-ion batteries are mainly responsible for providing lithium-ion. At present, the common cathode materials are $LiCoO_2$, $LiMn_2O_4$, $LiNiO_2$, ternary composite cathode materials and their modified varieties [23]. The structural instability, high cost, and non-environmental friendliness of cobalt materials make materials attractive for Li-ion batteries [24].

Over the last two decades there has been intensive research in improving the overall performance of Li -ion batteries. Among the different components of the battery mechanism one of the main foci has been alternative cathode materials. The graphite anode currently used in Li-ion rechargeable batteries have a theoretical capacity of 370mAh/g, which is twice the theoretical capacity of the formerly used layered $LiCoO_2$ cathodes, and avoids the use of expensive and toxic cobalt. Varieties of positive materials have been developed and are available commercially. Cathode materials can primarily be categorized based on structure types. $LiCoO_2$, $LiNiO_2$, Li_2MnO_3, $LiNi_{1-x}Co_xO_2$, $LiNi_{1/3}Mn_{1/3}Co_{1/3}O_2$ etc. have the olivine structure, and $LiMn_2O_4$ and spinel materials have a three- dimensional framework structure.

2.2.1. Lithium Cobalt Oxide ($LiCoO_2$)

Presently the lithium ion battery industry is dominated by the $LiCoO_2$ carbon anodes first introduced by Sony in 1991. This material was first reported by John Goodenough who recognized that this material had layered structure and that lithium could be removed electrochemically, thus making it a promising cathode material. $LiCoO_2$ has α-$NaFeO_2$ structure with O atoms present in a cubic closely-packed FCC arrangement, when lithium is completely removed; the oxygen layers rearrange themselves to give hexagonal close packing in form of CoO_2. Figure 3 below represents the layered structure of $LiCoO_2$.

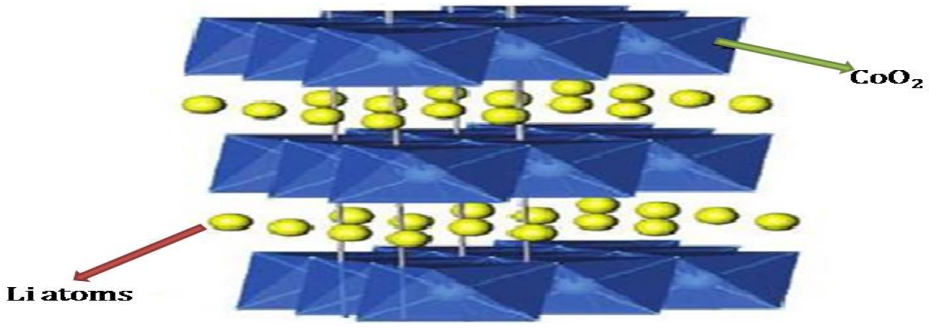

Figure 3: Layered structure of $LiCoO_2$ **[25]**.

This material shows an initial discharge capacity of 140 mAh/g at an average voltage of 3.7V. Cho et al showed that the capacity can be improved by coating a metal oxide or phosphate on the surface of the $LiCoO_2$ particles. They found that the capacity could be increased from 140 mAh/g to 170 mAh/g when cycled between 2.75 V and 4.4V without capacity fade over 70 cycles. Also improvement was shown in the cyclability for this material when coated with metal oxides such as Al_2O_3.

Though $LiCoO_2$ cathode material is leading the lithium-ion battery market, there is limited availability of cobalt, thereby making it an expensive material. A lot of research is being done to find a probable replacement for Co with materials that are abundant and that are environmental friendly such as Ni, Mn, Fe and Cr etc. Also, since $LiCoO_2$ capability various materials are being researched which form solid solution with $LiCoO_2$ such as $LiNiO_2$-Li_2MnO_3-$LiCoO_2$ [25], $LiCoO_2$-Li_2MnO_3 [26], $LiNi_{1/2}Mn_{1/2}O_2$-Li_2MnO_3-LiCoO2 [27, 28], $LiNiO_2$-$LiCoO_2$ [29]. The high specific energy of this battery type makes it very popular for mobile phones, notebooks, tablets and digital cameras. The cathode is made of cobalt oxide and the anode of carbon graphite. The main disadvantages are a short useful life, low thermal stability, and limited specific power.

2.2.2. Lithium Manganese Oxide ($LiMnO_2$)

Along with its counterparts such as $LiNiO_2$ and $LiCoO_2$, this material has also been researched a lot over the last decade mainly for its prospects of providing not only a low-cost but also an environmentally benign cathode material [30, 31]. However, in spite of these advantages $LiMnO_2$ was never available cathode mainly because this material is unstable at elevated temperatures and cannot be synthesized by the same methods as used for materials like NaMnO. One of the successful attempts for synthesis was accomplished by Na^+ ion exchange [31] and by low temperature methods such as hydrothermal synthesis [30]. Even when $LiMnO_2$ structure $LiMn_2O_4$ is synthesized, it tends to revert itself to form a more stable spinel. Though initially was not desired, $LiMn_2O_4$ has proven to be available cathode material mainly because of the three-dimensional framework which adds stability to the structure during

delithiation. Additionally, unlike $LiNiO_2$ and $LiCoO_2$ exothermically with the electrolyte making it potentially safer than $LiNiO_2$ following figure shows a comparison between $LiMnO_2$/$LiMn_2O_4$ structures.

The tunnel like structure for $LiMn_2O_4$ allows lithium to move out of the structure without collapse even under high charge/discharge rates. However, the main drawback of this material is the nature of its discharge which can be divided into 2 regions: one at 4V and the other at 3V range with a capacity of 150 mAh/g. After the 4V plateau, it is possible for one or more lithium ions to be present because the reaction is not in equilibrium leading to Jahn-Teller distortion which is associated with the phase transition from cubic to a tetragonal crystal structure. Additionally, this material also tends to self-discharge at elevated temperature [33]. There have been several attempts in improving the capacity fade by coating the material with different oxides [34-36] and also techniques like cation substitution and surface treatments have been employed to address the problem with self-discharging. The components of this battery form a tridimensional structure that allows a better flow of electrons in the electrodes generating a smaller internal resistance and a better current management.

2.2.3. Lithium Nickel Manganese Cobalt Oxide ($LiNiMnCoO_2$ or NMC)

The NMC Li-ion battery uses a cathode combination of nickel, manganese, and cobalt. Nickel has high specific energy but poor stability, while manganese forms a strong structure but offers a low specific energy; making this combination complementary. These types of batteries have good performance and high specific energy. Also, it has the lowest self-heating rate, making it a good candidate for electric vehicles.

2.2.4. Lithium Iron Phosphate ($LiFePO_4$)

This chemistry can withstand high temperatures; hence it is stable in overcharge or short circuit conditions. Among its advantages it is possible to mention the environmental benignity, high temperature capability and potential low-cost synthesis.

2.2.5. Lithium Nickel Cobalt Aluminium Oxide ($LiNiCoAlO_2$)

This battery provides great performance in terms of a long lifetime and high power density. Given this advantage, NCA batteries result as a good candidate for electric power trains. However, it presents a safety and security risk when used in large quantities, increasing its cost synthesis.

2.2.6. Lithium Titanate ($LiTi_5O_{12}$)

This type of cell has a good electrochemical stability. Main advantages of this cell type are: fast recharge time, high efficiency, and long lifetime. Also, this type of battery is considered to be safer. Furthermore, it has a wider operating temperature range.

2.2.7 $LiNi_{1-y}Mn_yO_2$

Lithium nickel manganese oxides have been of great interest among researchers for advanced lithium-ion batteries and as a possible replacement for $LiCoO_2$ [28, 37-45]. Material compounds of this type were first reported by Dahn et al in 1992 [39]. They reported a solid solution for y=0.5 but a deterioration of the electrochemical behavior with increasing manganese content.

The main advantage of this material is the fact that there is no Co content which is very expensive and a toxic compound compared to Ni and Mn. The most successful material of this group has been $LiNi_{1/2}Mn_{1/2}O_2$. Saphr et al [40] repeated the work of Dahn and showed maximum solubility of 0.5Mn, he was the first one to report the electrochemical behavior on $LiNi_{1/2}Mn_{1/2}O_2$ material. They showed that the Ni and Mn were present in $^{+2}$ and $^{+4}$ oxidation states rather the $^{+3}$ and $^{+3}$ respectively through XPS and magnetic data and also that this material showed a capacity of 150 mAh/g falling to 125 mAh/g after 25 cycles and to 75 mAh/g after 50 cycles when prepared at 700 °C

The active element in this material is Ni, which cycles between the Mn^{+2} and Mn^{+4} valences states, while manganese remains as Mn^{+4}, thereby leaving with no concern for Jahn-Teller distortion associated with the Mn^{+} ion. This material is commonly referred as “550” material (0.5 Ni, 0.5 Mn, 0 Co) was rediscovered by Ohzuku in 2001 [38]. Ohzuku reported an initial

discharge capacity of 150 mAh/g for 30 cycles using top-up charging at 4.3V when prepared at 1000 C. Recently, Ohzuku reported the cycle tests of lithium cells with $LiNi_{1/2}Mn_{1/2}$ O2operated in voltages of 2.5-4.5V of about 200mAh/g of rechargeable capacity for 30 cycles [37].

2.3 Anode Materials

Anode materials are the negative electrode in lithium-ion batteries and are paired with cathode materials in a lithium-ion cell. The anode materials in lithium-ion cells act as the host where they reversibly allow lithium-ion intercalation /deintercallation during charge / discharge cycles. General criteria for selection of suitable intercalation-based anode materials include (i) low first cycle irreversible loss, (ii) high coulombic efficiency, (iii) fast lithium-ion diffusion into and out of the anode, (iv) high ionic and electronic conductivity, (v) minimum structural changes upon charge and discharge, (vi) high specific capacity (mAh/g), and (vii) the ability to form and maintain a stable SEI (Solid Electrolyte Interface) layer upon cycling.

2.4 Electrolytes

In batteries, electrochemical processes are responsible for storage and release of electric energy (charging and discharging). To transport the electric charge between the electrodes, electrolytes are necessary. Electrolytes can be liquid, but polymer- or solid-state electrolytes exist. Ionic liquids are interesting electrolytes for a series of electrochemical cells, due to their outstanding properties, like:

- High electrochemical stability against reduction and oxidation (wide electrochemical window)
- Electric conductivity: for pure ionic liquids lies at up to 27 mS/cm at 25 ^{o}C, for mixtures it can reach up to 70 mS/cm.
- Thermal stability
- Low vapour pressure
- Low flammability

Many manufacturers are represented with their new developments on numerous cell types in market, but there is no unified state of the art technical design. That means, each particular electrode material will set very strict restrictions on specific properties of electrolytes, that should be combined with it. The additional demand for further development stems from the fact, that there are serious safety issues coupled to the use of some batteries.

2.5 Separators

Separators are essential components of Li-ion batteries. In fact, separators are commonly used in most electrochemical systems with liquid electrolyte, including fuel cells, capacitors and various kinds of batteries based on different chemistry. The separator in a Li-ion battery plays the critical roles to avoid direct physical contact between the cathode and anode, and prevents short circuit to occur. At the same time, the separator allows lithium ions in the electrolyte to pass through it. The separators must be chemically stable and inert in contact with both electrolyte and electrodes. At the same time, it is required to be mechanically robust to withstand the tension and puncture by electrode materials and the pore size should be less than 1 μm. Although various separators, including microporous polymer membranes, nonwoven fabric mats and inorganic membranes have been explored, the microporous polyolefin materials based polymer membranes are dominantly used in commercial Li-ion batteries with liquid electrolyte.

2.6 Battery lifetime

Rechargeable battery life is typically defined as the number of full charge-discharge cycles before significant capacity loss. Inactive storage may also reduce capacity. Manufacturers' information typically specify lifespan in terms of the number of cycles (e.g., capacity dropping linearly to 80% over 500 cycles), with no mention of chronological age. On average, lifetimes consist of 1000 cycles, although battery performance is rarely specified for more than 500 cycles. This means that batteries of mobile phones, or other hand-held devices in daily use, are not expected to last longer than three years. Some batteries based on carbon anodes offer more than 10,000 cycles. As a battery discharges, its voltage gradually diminishes. When depleted below the protection circuit's low-voltage threshold (2.4 to

2.9V/cell, depending on chemistry) the circuit disconnects and stops discharging until recharged. As discharge progresses, metallic cell contents plate onto its internal structure, creating an unwanted discharge path.

It is also important to maintain safe operating temperature to avoid thermal destruction. For lithium-ion batteries the best operating temperatures are in the range between 25°C and 40 °C [8]. To avoid the occurrence of an excessive temperature rise [9] leading to the degradation in their lifetime or even worse to the thermal runaway phenomenon, local temperature of lithium-ion batteries should be carefully monitored.

Defining battery life via full discharge cycles, is the industry standard, but may be biased, since full depth of discharge (DoD)/recharge may itself diminish battery life, compared to cumulative Ah partial discharge/charge performance.

2.7. Mechanisms of Constructing Lithium Ion Battery

A Li- ion battery is constructed by connected basic Li- ion cells in parallel (to increase current), in series (to increase voltage) or combined configurations. Multiple battery cells can be integrated into a module. Multiple modules can be intergrade into a battery pack. For example, the 85 kWh battery pack in a typical Tesla car contains 7104 cells. Typically, a basic Li- ion cell consists of a cathode (positive electrode) and an anode (negative electrode) which are contacted by an electrolyte containing lithium ions. The electrodes are isolated from each other by a separator, typically microporous polymer membrane, which allows the exchange of lithium ions between the two electrodes but not electrons. In addition to liquid electrolyte, polymer, gel, and ceramic electrolyte have also been explored for applications in Li- ion batteries.

Figure illustrates the basic operating principle of a typical Li- ion battery cell. The basic design of Li- ion cells today is still the same as those cells Sony commercialized two decades' age, although various kinds of electrode materials, electrolyte, and separators have been explored.

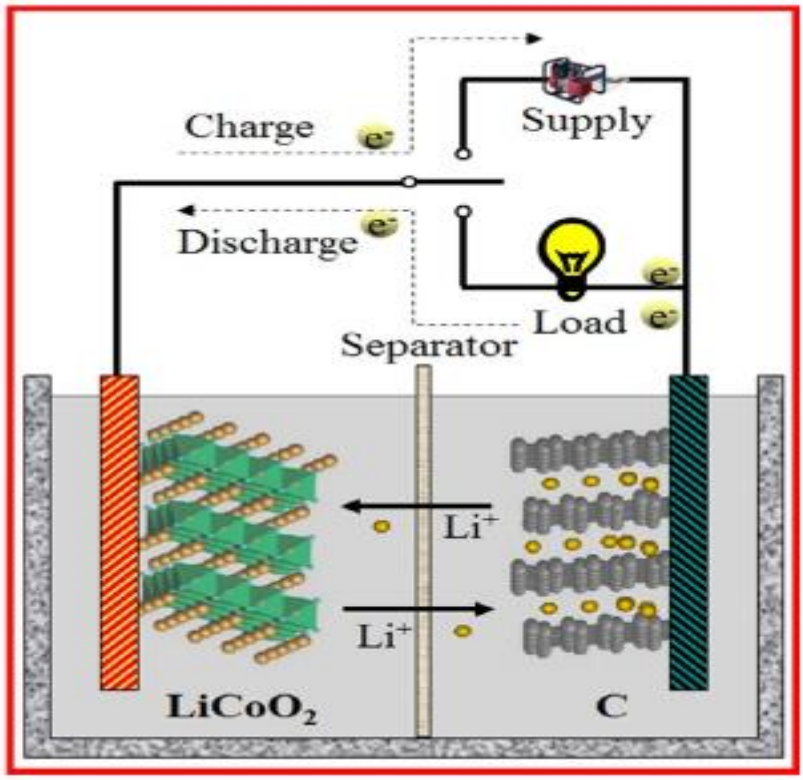

Figure 4. Illustration to show the basic components and operation principle of a Li- ion cell. Reproduced with permission **[46]**.

The commercial cells are typically assembled in discharged state. The discharged cathode materials (e.g., $LiCoO_2$, $LiFePO_4$) and anode materials (e.g., carbon) are stable in atmosphere and can be easily handled in industrial practices. Yohsino made a significant contribution to the commercial production of Li-ion batteries by using discharged electrode materials in full cells for the first time.

During charging process, the two electrodes are connected externally to an external electrical supply. The electrons are forced to be released at the cathode and move externally to the anode. Simultaneously the lithium ions move in the same direction, but internally, from cathode to anode via the electrolyte. In this way the external energy are electrochemically stored in the battery in the form of chemical energy in the anode and cathode materials with different chemical potentials. The opposite occurs during discharging process: electrons move from anode to the cathode through the external load to do the work and Li ions move from anode to the cathode in the electrolyte. This is also known as "shuttle

chair" mechanism, where the Li ions shuttle between the anode and cathodes during charge and discharge cycles.

Electrochemical reactions at the two electrodes released the stored chemical energy [46]. The total Gibbs free energy change due to the electrochemical reactions on the two electrodes is determined by the electrode materials selected. Given the overall electrochemical reaction and charges transferred, one can estimate the theoretical cell voltage ($\Delta E = -\Delta G/nF$). The performance of Li- ion batteries can be evaluated by a number of parameters, such as specific energy, volumetric energy, specific capacity, cyclability, safety, abuse tolerance, and the discharge/charging rate. Specific energy (Wh/kg) measures the amount of energy that can be stored and released per unit mass of the battery. It can be obtained by multiplying the specific capacity (Ah/kg) with operating battery voltage (V). Specific capacity measures the amount of charge that can be reversibly stored per unit mass. It is closely related to number of electrons released from electrochemical reactions and the atomic weight of the host.

Cyclability measures the reversibility of the Li- ion insertion and extraction processes, in terms of the number of charge and discharge cycles before the battery loses energy significantly or can no longer sustain function of the device it powers. Practically, the cycle life of Li-ion batteries is affected by depth of discharge (DOD) and state of charge (SOC), as well as operating temperature, in addition to the battery chemistry. Cycle life is enhanced with shallow DOD cycles and less SOC swing, and avoiding elevated temperature. Li dendrite formation on graphite anode can occur at low-temperature charge which should be avoided. Safety requirement is very high for Li-ion batteries with multiple cells. Battery management systems (BMS) are typically employed in battery cells/packs/modules to prevent any possible thermal runaway. For example, in the case of battery cell failure inside a battery pack, the BMS could detect and isolate the particular cell.

2 .9. COMSOL Multiphysics

COMSOL Multiphysics is finite element simulation software. It is able to couple different kind of physics by using modules such as electrical, mechanical, fluid and chemical. One of

these modules is called Batteries & Fuel Cells and can simulate the heat generation of a Lithium-Ion battery. This module allows modeling the underlying electrochemical behavior in the electrodes and electrolytes. In the following, we present the modeling of the battery of the Cal Poly electric race car inorder to determine the heat behavior of the battery pack in a discharge case. For a battery manufacturer, modeling and simulations improve the design of cells and modules. By describing the involved processes on a detailed level in a model, the designer may apply different hypotheses and relate these with the observed and simulated behavior of a given cell. This results in the intuition for a system that is required for making vital improvements. This COMSOL Multiphysics is used to evaluate the efficiency of battery.

2.9.1 COMSOL Model of the Cell

Two COMSOL Multiphysics modules are necessary to figure out the heat generation of the battery. The first, Batteries and Fuel Cells, simulates the chemical reaction between the anode, the cathode and the separator in one dimension. The second, Heat Transfer in Solids simulates the heat conduction in all the battery. The coupling between these two physics is illustrated by the Figure . The chemical reaction is dependent on the temperature distribution; the temperature distribution evolves due to the chemical heat generation.

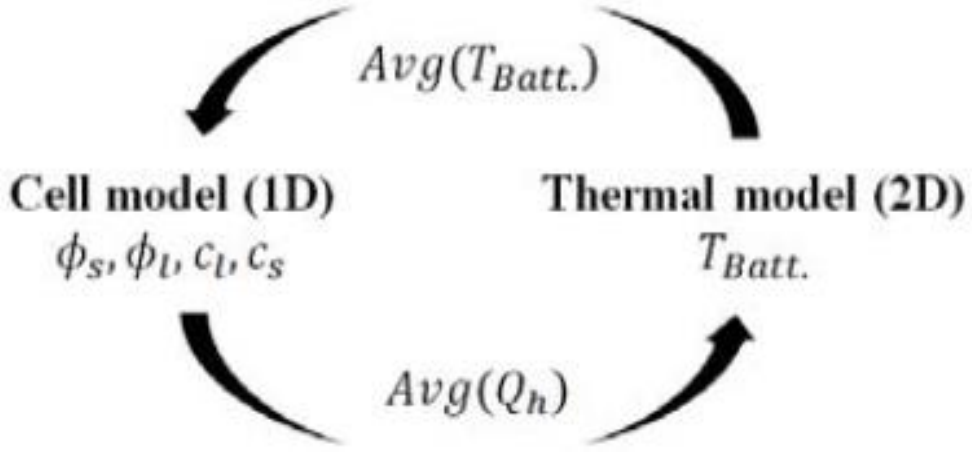

Figure 5. Coupling variables in the thermal modelingof a Li-Ion battery cell.

2.9.2 COMSOL model of the battery pack

The electric race car battery pack is composed of 40 battery cells connected together with two long screws. To model the battery pack, the current collector tabs will be neglected as the closure and the two folds on each side of the battery.

2.9.3 Battery pack geometry

The 3D model has been drawn on Solid Works and then imported on Comsol in ".STEP" format. It includes from 10 to 40 cells inorder to see the evolution of the heat versus the length of the pack. For the sake of simplicity, Figure 8 shows a pack of ten battery cells.

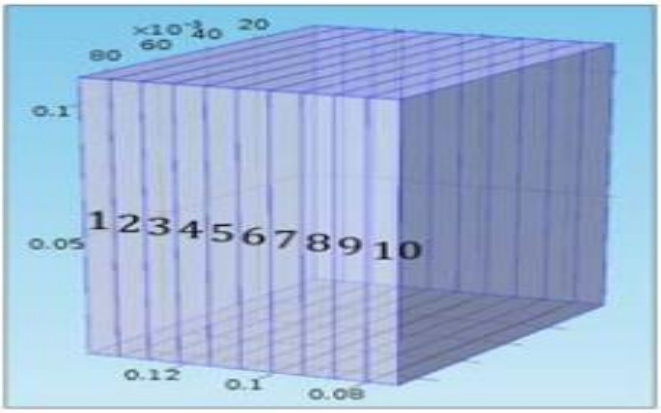

Figure 6. Pack of ten elements

Chapter 3: Materials and Methods

3.1 Materials and Equipment's

3.1.1. Materials and chemical

Lithium nitrate ($LiNO_3$), Nickel nitrate ($NiNO_3$), manganese nitrate tetrahydrate ($Mn(NO_3)_2.H_2O$, urea ($CO(NH_2)_2$, carbon black, lithium metal (50µm thick), lithium hexa fluorophosphate ($LiPF_6$), ethylene carbonate (EC), diethyl carbonate (DEC), and dimethyl carbornate (DMC) were purchased from Sigma-Aldrich and used without further purification. Aluminum foil (50µm thick) was obtained from MTI Corporation.

3.1.2 Equipments

X-ray diffraction (XRD), Scanning electron microscopy (SEM), Thermo-gravimetric analysis (TGA), Beaker, Magnetic stirrer, Hot plate, Furnace and Grinding were used.

3.2. Methods of the Experiment

$LiNO_3$ (0.550 gm, 0.016 mol.), $Mn(NO_3)_2{\cdot}4H_2O$ (4.00 g, 0.032 mol.), $Ni(NO_3)_2{\cdot}6H_2O$ and urea ($(NH_2)_2CO$) (1.435 gm, 0.047 mol.) were used as precursors. All nitrates were dissolved in deionised water (20.00 ml) and kept under magnetic stirring for 30 min at room temperature and until the starting materials were completely dissolved. The solution was then heated on hot-plate for 30 min. The combustion reaction is a chemical reaction that depends on the fuel material and the purity of the starting reactants. Figure illustrated steps of procurer the combustion reaction.

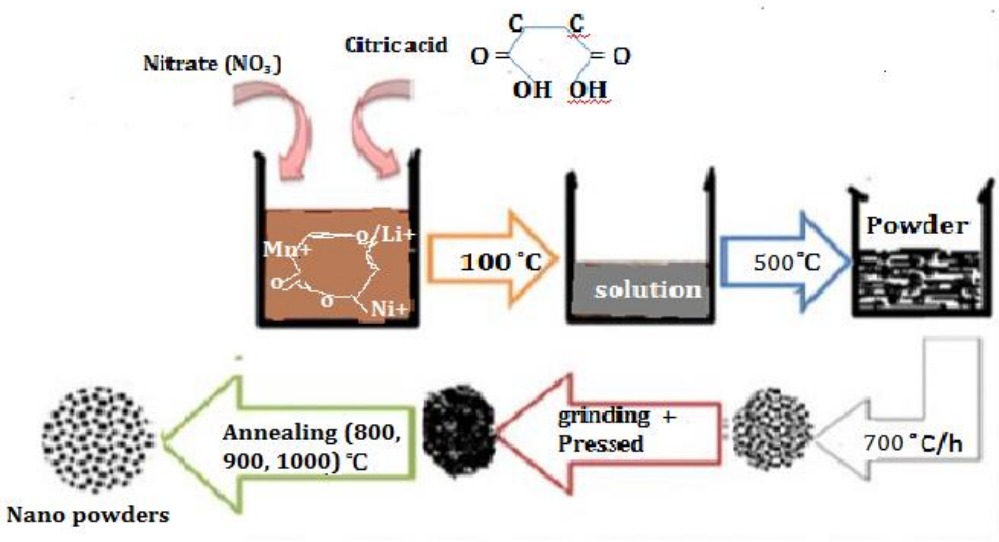

Figure 7. Schematic of combustion reaction

To obtain the maximum energy released during the combustion synthesis process, the stoichiometric compositions of the redox mixtures for the combustion reaction are calculated using the total oxidizing (O) and reducing (R) valencies of the components. The equivalent ratio, Re = O/R, was kept unity (O/R = 1). The atoms H, C, Li, Mn, and Ni are considered reducing agents with valencies +1(H), +4(C), +1(Li), +2(Mn), and +2(Ni), respectively. The oxygen atom is considered an oxidizing agent with a valency of -2. For the pristine $LiMn_2O_4$ sample synthesis the stoichiometric reaction equation can be put as [52, 53]:

$$LiNO_3+2Mn\ (NO_3)_2+4.2NH_2\text{-}CO\text{-}NH_2 \rightarrow LiMn_2O_4+6.7N_2+\ 4.2CO_2+8.4H_2+3.4O_2$$

Accordingly, based on the stoichiometric ratios, appropriate masses of the precursor materials (see Table 1) were dissolved into20 ml of deionised water in a 100 mL beaker and stirred at ambient temperature for about 30 min to obtain homogeneously mixed solution. After that, the precursor solution was introduced into a furnace, preheated at 500 °C and the exothermic reaction took place and completed within 10 minutes to obtain a black powdered product. In the synthesis mechanism, essentially there are about three steps, first the solution boils and undergoes dehydration followed by decomposition, and it involves generating traces of NO_x and other combustible such as NH_3 and N_2H_4, and finally the

formation of metal oxides. In order not to be exposed to the toxic gases being released, we have added extra 10 minutes after completion of the reaction to allow possible toxic NO_x gases completely leave from the furnace [52]. And then finally, the product powder was collected and calcined at 700 ℃ for 10 h to form spinel $LiMn_2O_4$ crystal structure. To investigate the effect of Ni ion on the structural and electrochemical properties of $LiMn_2O_4$ cathode materials, Ni substituted samples (with Ni-ion concentration of 0.125, 0.25, 0.375, and 0.5) were prepared under atmospheric pressure and then calcined at 700℃ in air for 10h. The voluminous and foamy combustion ash was easily milled to obtain the final $LiNi_xMn_{2-x}O_4$ cathode materials.

Table 1 Mass of the precursor materials in gram calculated according to the stoichiometric ratio.

Sample	Mass of precursor materials used in the synthesis (gm)			
	$LiNO_3$	$Mn(NO_3)_2.4H_2O$	$Ni(NO_3)_2{\cdot}6H_2O$	$(NH_2)_2CO$
$LiMn_2O_4$	0.550	4.000	0	1.435
$LiNi_{0.125}Mn_{1.875}O_4$	0.550	3.750	0.370	1.435
$LiNi_{0.25}Mn_{1.75}O_4$	0.550	3.500	0.750	1.435
$LiNi_{0.375}Mn_{1.625}O_4$	0.550	3.250	1.120	1.435
$LiNi_{0.5}Mn_{1.5}O_4$	0.550	3.000	1.500	1.435

The structural properties of the samples were investigated by X-ray diffraction analysis using a PANalytical X'Pert PROP W3040/60 X-ray diffractometer with Fe-filtered Cu-Kα (λ =1.5479026 nm) monochromated radiation source. Data were collected in the 2Θ range of 5˚-70˚ at a scan rate of 2˚ /min. The morphology of the products was obtained using a high-resolution scanning electron microscope (JEOL, JSM-7600F, operated at an accelerating voltage of 5 kV).

3.3. Electrochemical characterization

Electrochemical cells were configured in the following way; coin cells of 2032 were assembled using lithium metal as anode, Celgard 2400 as separator,1 M solution of $LiPF_6$ in 50:50 (v/v) mixture of ethylene carbonate (EC) and diethylene carbonate (DEC) as the electrolyte. The cathode was made through a slurry coating procedure from a mix containing active material powder, conducting black and poly (vinylidene fluoride) binder in N-methyl-2-pyrrolidone in the proportion 80:10:10, respectively. The slurry was coated over aluminium foil and dried at 120 ℃ overnight for 12 h. 18 mm diameter slurry-coated aluminium foils electrodes were punched out and used as cathode.

Thermal analysis of the powder sample was made using the thermo-gravimetric analyzer (TGA) from lenses German. The heating rate was set at 10 ℃/min while atmospheric pressure was maintained during the measurements. The aim of the thermal analysis is to find the optimum temperature at which elimination of contaminants and phase formation along with crystallization take place.

Chapter 4: Results and Discussion

This chapter deals with the analysis, discussion and the results of the thesis. The morphological and structural characterization of $LiNi_xMn_{2-x}O_4$ were analyzed.

4.1 Morphology and structural characterization

The morphologies of the as-prepared $LiNi_xMn_{2-x}O_4$ crystalline materials were examined by SEM. Figure a-d shows SEM morphological structure of $LiMn_2O_4$, $LiNi_{0.125}Mn_{1.875}O_4$, $LiNi_{0.25}Mn_{1.85}O_4$ and $LiNi_{0.375}Mn_{1.625}O_4$ samples, respectively. The SEM structural analysis display that the synthesized spinel $LiNi_xMn_{2-x}O_4$ (x = 0, 0.125, 0.25, 0.375) cathode materials have spherical or spherical like morphology with particle size of micrometers. Generally, spinel $LiMn_2O_4$ cathode materials with spherical morphology showed Zero stress deviation on structures during charge-discharge reaction because the Jahn-Teller distortions from a certain side can be counteracted by the opposite side of the spherical particles [13]. The formation of microsized spherical particles is able to enhance the cycle life time of all the as-synthesized cathode materials including the pristine $LiMn_2O_4$. The estimated particle size range for the compositions for x=0.125, x=0.25 and x = 0.375 are 3.4–8 μm, 4.2–10 μm, and 6.5–10 μm, respectively.

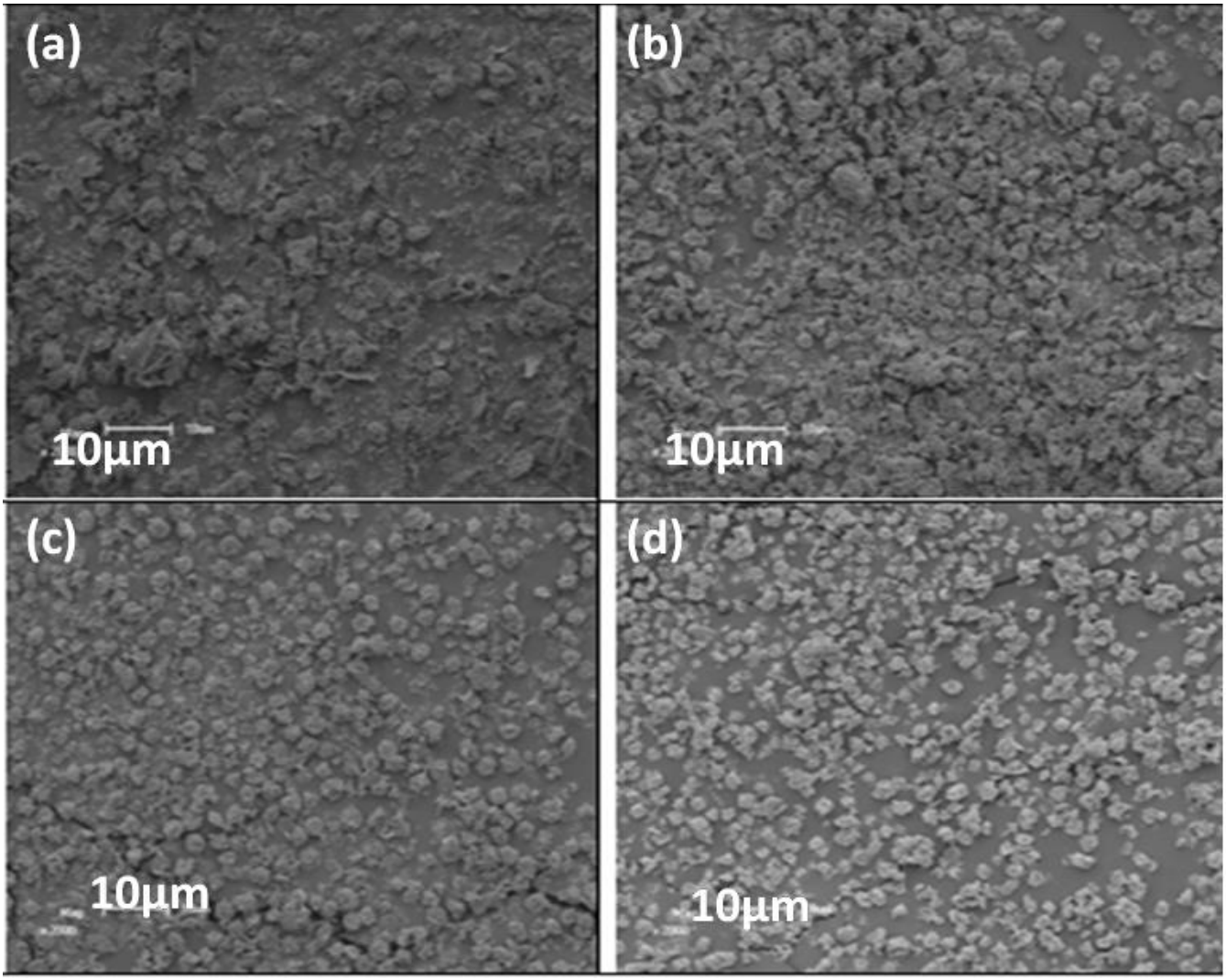

Figure 8.Top-view SEM micrographs of the products (a) $LiMn_2O_4$ (b) $LiNi_{0.125}Mn_{1.875}O_4$ (c) $LiNi_{0.25}Mn_{1.75}O_4$ and (d) $LiNi_{0.375}Mn_{1.625}O_4$.

4.2. XRD structural characterization

The structural properties of the $LiNi_xMn_{2-x}O_4$ crystalline materials were analyzed by X-ray diffraction. Figure represents a typical X-ray diffraction pattern of as synthesized samples. The examination of the diffraction patterns confirms that all recognizable reflection peaks including (111), (311), (400), (511) and (440) can be clearly indexed to the single phase of the spinel cubic structure of $LiMn_2O_4$ with space group Fd3 m and with some impurity peaks. There is increase crystal structure after the Ni substitution. This indicates that the Ni^{2+} substituting ions have seated at Mn^{3+} site in $LiMn_2O_4$ and thus no other phase is formed. When Ni substitution increase the peaks are become very sharp, and this indicating a high crystallinity of the powders.

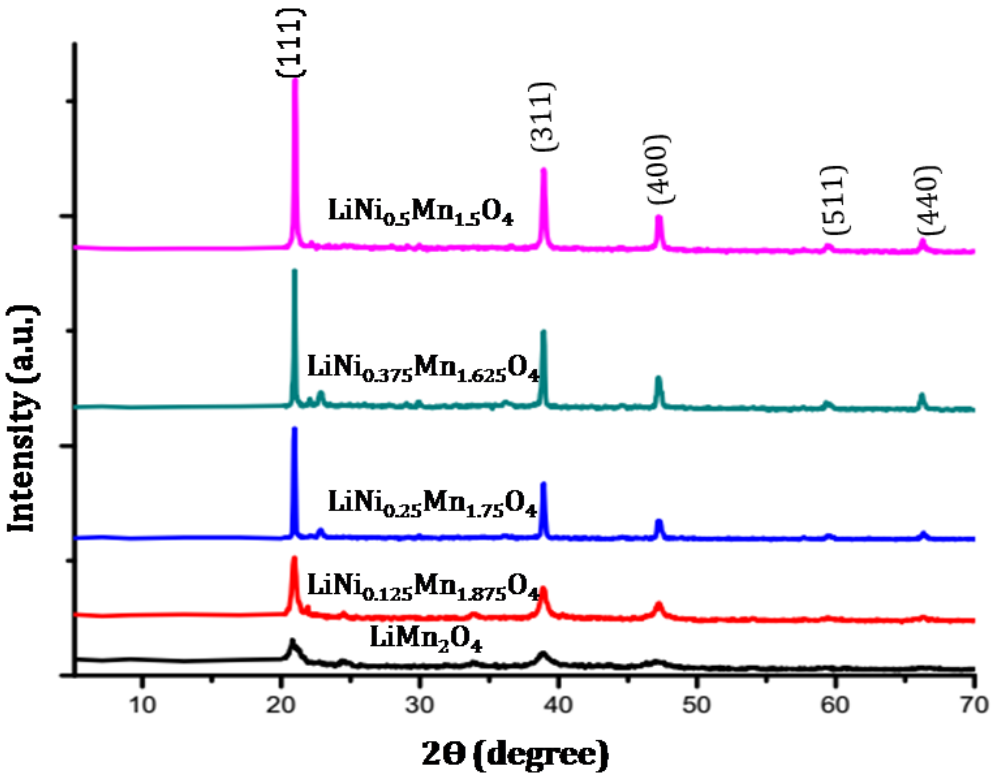

Figure 9. X-ray pattern of synthesized $LiNi_xMn_{2-x}O_4$ (x= 0, 0.125, 0.25, 0.375, and 0.5) spinel cathode materials

Table 2 compares the lattice parameters (a-value/Å and unit cell volume/$A^{\circ 3}$) of the pristine and Ni-doped spinel materials. The calculated values from the XRD follows same trend with the ab initio calculation. As the amount of nickel is increased, the lattice parameter is decreased. This is expected considering that there is increase in the concentration of small Mn^{4+} (0.53 Å) ions in the spinel structure as big Mn^{3+} (0.645 Å) ions are substitutes by smaller Ni^{3+} (0.53 Å) ions.

Table 2 Structural parameters obtained for the $LiNi_xMn_{2-x}O_4$ (x = 0, 0.125, 0.25, 0.375, and 0.5) samples from both XRD (Rietveld refinement) and DFT calculations.

Sample	XRD Rietveld refinement		DFT calculation	
	a (Å)	Unit cell volume ($Å^3$)	a (Å)	Unit cell volume ($Å^3$)
$LiMn_2O_4$	8.2242	556.264	8.3232	576.595
$LiNi_{0.125}Mn_{1.875}O_4$	8.2231	556.041	8.3228	576.512
$LiNi_{0.25}Mn_{1.75}O_4$	8.2099	553.367	8.28	567.664
$LiNi_{0.375}Mn_{1.625}O_4$	8.2086	553.105	8.26	563.559
$LiNi_{0.5}Mn_{1.5}O_4$	8.1757	546.480	8.24	559.476

4.3 Electrochemical Characterization and results

Generally, the theoretical capacity,C_T, can be expressed as follows [62]:

$$C_T = 26.8\frac{p}{M}, \quad (1)$$

where $\boldsymbol{p}$ and $\boldsymbol{M}$ denote the number of Mn(III) and the molecular weight of ion-doped $LiMn_2O_4$, respectively. Employing Eq. (1), the theoretical capacity of $LiNi_xMn_{2-x}O_4$ is found to be 148, 132.2, 115.6, 98.3, and 80.3 $mAhg^{-1}$ for x = 0, x = 0.125, x = 0.25, x = 0.375, and x = 0.5, respectively. The trend of the first cycle discharge capacity of the $LiNi_xMn_{2-x}O_4$ cathode materials in relation to the Nickel content is displayed in Figure 4 a. The first cycle discharge capacity of pristine $LiMn_2O_4$ and $LiNi_{0.125}Mn_{1.875}O_4$ samples did not much vary significantly.

Also, as displayed in Figure 4 b, the calculated lattice parameter of $LiNi_{0.125}Mn_{1.875}O_4$ (8.3228 Å parameter of pristine $LiMn_2O_4$) is almost equal to the lattice (8.3232 Å). These experimental and theoretical results indicate that both pristine $LiMn_2O_4$ and small Ni-content-doped $LiNi_{0.125}Mn_{1.875}O_4$ samples exhibit high first cycle discharge capacity and larger lattice parameters compared with other high Ni-content doped samples. The larger the lattice parameter, the easier the Li ions can more freely [32–34], thereby increasing the discharge capacity. As expected, beyond x = 0.125 (in our case for x = 0.25, 0.375, and0.5) the first cycle discharge capacity of the doped $LiMn_2O_4$ cathode material becomes much less than that of the pristine $LiMn_2O_4$. A higher degree of Ni doping can therefore be correlated with a decreased lattice parameter, which in turn leads to a lower discharge capacity. This finding indicates that the discharge capacity is not only correlated exclusively to the molecular weight of ion-doped $LiMn_2O_4$, but also to its lattice parameter.

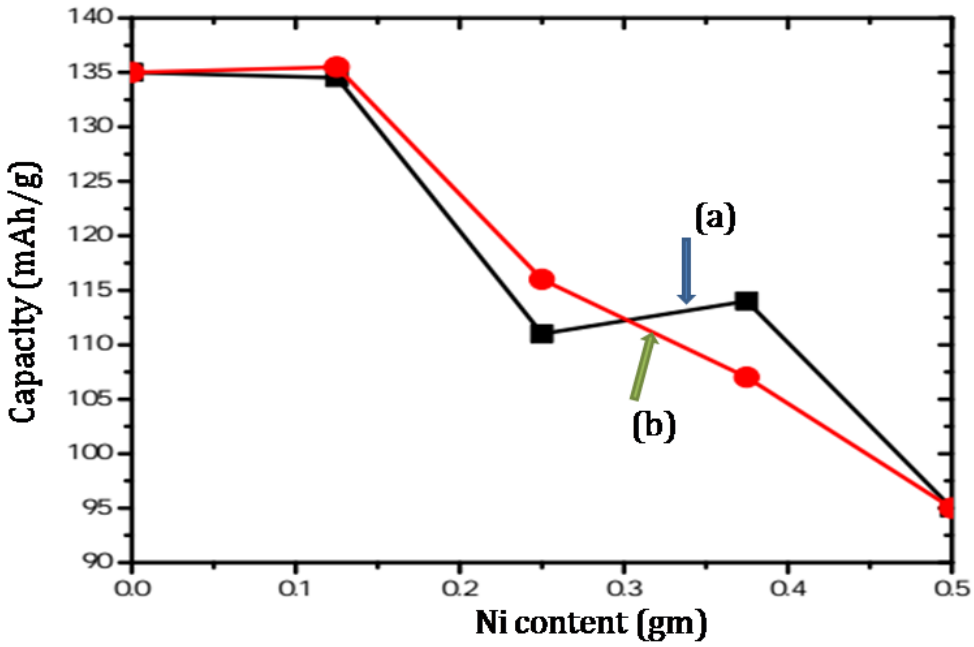

Figure 4(a) First cycle discharge capacity of $LiNi_xMn_{2-x}O_4$ and (b) the calculated lattice parameter of the composition $LiNi_xMn_{2-x}O_4$ (x= 0, 0.125, 0.25, 0.375, 0.5).

Figure (a) represents the change in discharge capacity (50th cycle discharge capacity/first discharge capacity) for the $LiNi_xMn_{2-x}O_4$ cathode materials. Compared with the pristine $LiMn_2O_4$ cathode material, the $LiNi_{0.125}Mn_{1.875}O_4$ composition did not improve the cyclability, whereas the other doped spinel compositions do retain their initial capacities for many cycles; for example, Nickel doped compositions $LiNi_{0.25}Mn_{1.75}O_4$, $LiNi_{0.375}Mn_{1.625}O_4$, and $LiNi_{0.5}Mn_{1.5}O_4$, respectively, retain 1.5, 1.6, and 1.3 times that of pristine $LiMn_2O_4$. It is apparent that the samples with Ni-ion concentration of x = 0.375 exhibit higher capacity retention about 85% after 50 cycles. The enhanced cyclability of the sample $LiNi_{0.375}Mn_{1.625}O_4$ in the present study is primarily attributed to the optimum Ni ion doping which results in stabilizing the spinel structure. As shown in Figure b, an increase in Ni-dopant corresponds to more negative intercalation energy which implies easy Li-ion movement.

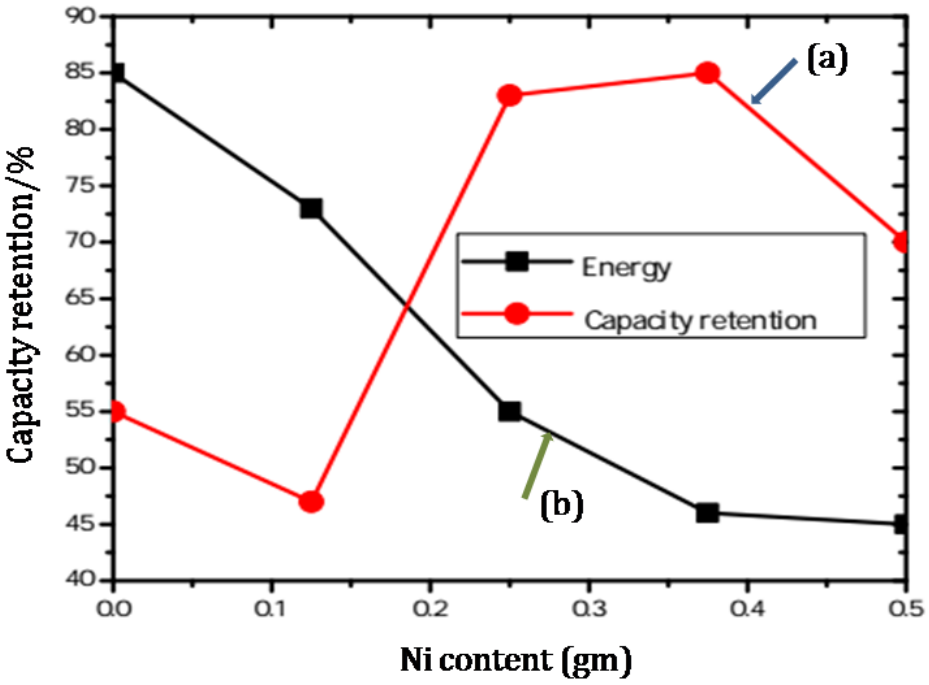

Figure 11 (a) Discharge capacity retention of $LiNixMn_{2-x}O_4$ after 50 cycles at C-rate = 0.2C, (b) the computational intercalation energy per Li atom.

4.4. Thermo-gravimetric Analysis (TGA)

The mass (weight) loss curve with temperature is analyzed by Thermo-Gravimetric Analysis (TGA). Figure shows the TGA and its derivative curves with a heating rate of 10 ℃/min in inert atmosphere. First order derivative of TGA curves reveals the temperature at which the maximum decrease of mass occurs. Three apparent weight loss at 96.5 ℃, 494 ℃ and 543 ℃ were observed, which might be attributed to the desorption of adsorbed water and decomposition of functional groups including hydroxyl and carboxylic groups respectively. The mass loss curve exhibited a continuous decrease of mass with temperature.

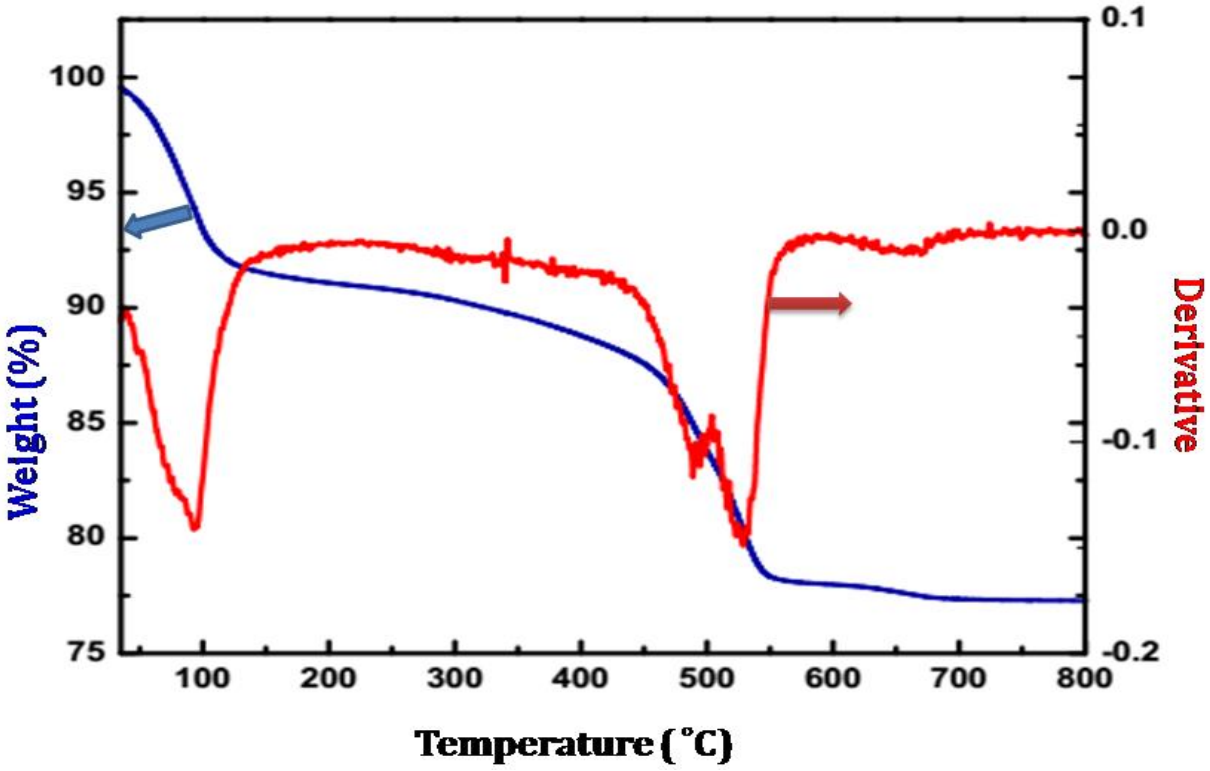

Figure 12 TGA curves with a heating rate of 10 ℃/min.

4.5 The COMSOL Multiphysics (MP) 3.5a model

4.5.1 The thermal effect on the cell voltage

The cell voltage provides more discharge capacity when it is placed in a better heat isolation environment (i.e. adiabatic condition). In a better isolated environment, the cell temperature increases faster during the 1 C discharge process which results in the higher diffusion coefficient for the binary electrolyte and reduces the diffusion limitations. Figure shows a comparison of the constant current discharge curves. The first load cycle differs from the rest significantly due to different initial values. For cycles 2 through 10 there is a gradual decrease of the battery voltage for each cycle.

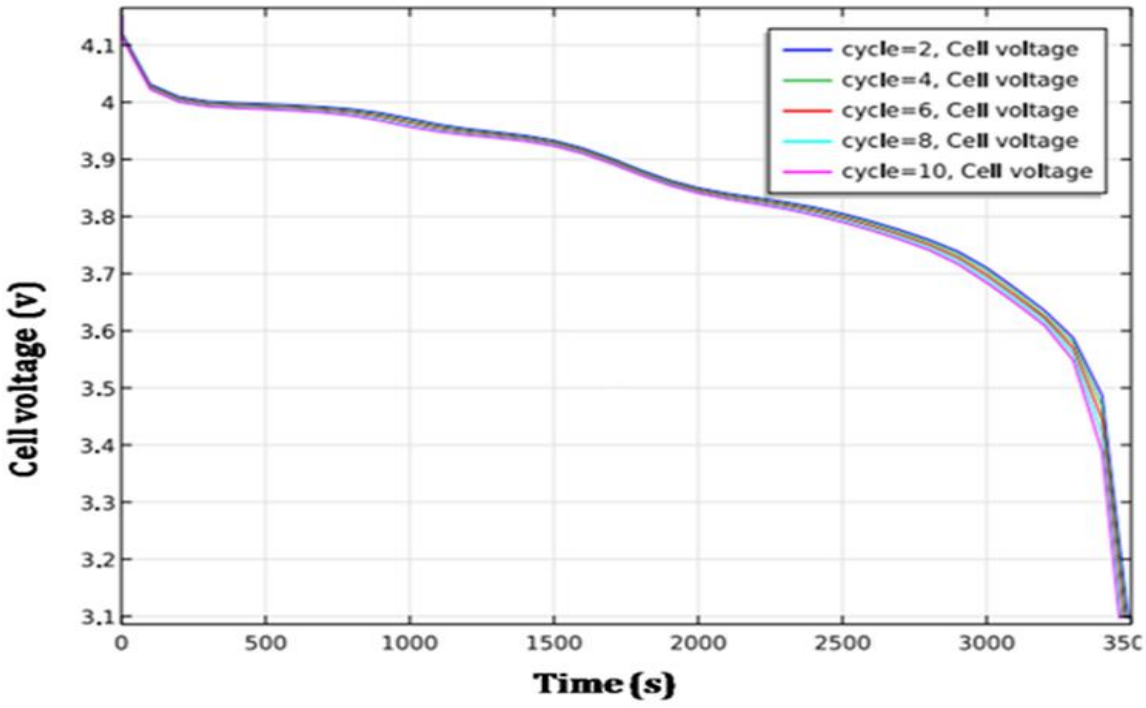

Figure 13: Discharge current comparison: battery voltage versus time for cycles 2, 4, 6, 8, and 10

4.5.2 Discharge Curves

A first modeling approach is to simulate discharge at various current densities and then display the discharge curves. The results show the capacity of the battery at different discharge rates. This model defines end-of-discharge as the time when the cell voltage drops below 3 V. **Figure** shows that the maximum discharge capacity of 17.5 Ah/m^2 is obtained for a current density of 1.75 Ah/m^2 (0.1 C). It can also be seen that the 3 V discharge capacity decreases slightly when applying a 1 C discharge current and dramatically when going above that. At 4 C, the battery delivers approximately 50% of the theoretical capacity before it reaches a cell voltage of 3 V.

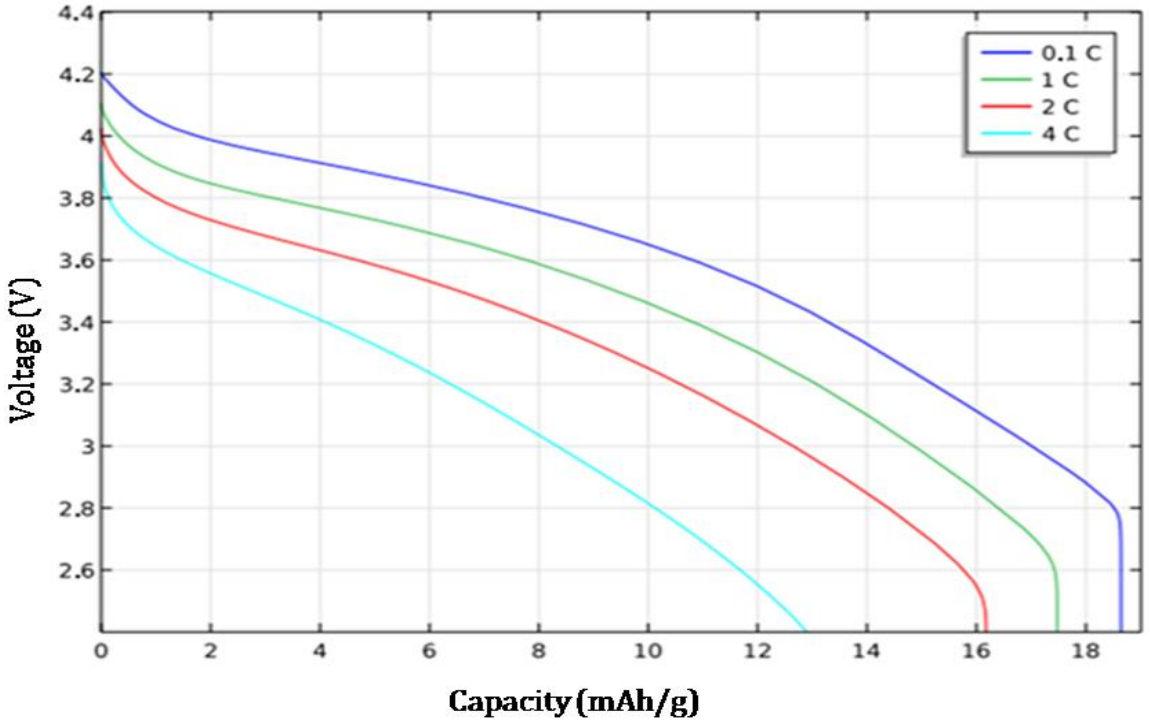

Figure 14 Discharge curves for various discharge rates.

Chapter 5: Conclusion

Pristine(LMO) and Ni-doped lithium manganese oxide ($LiNi_xMn_{2-x}O_4$) spinel cathode materials were successfully synthesized using metal nitrates and urea as precursors by solution combustion method. We studied the use of low nickel as a substituting for $LiMn_2O_4$ spinel cathode material for lithium ion battery. The samples were characterized by scanning electron microscopy (SEM), X-ray diffraction (XRD), Thermo-gravimetric analysis (TGA) and charge/discharge battery tester as well as using COMSOL Multiphysics software. The SEM analyzed structure display that the synthesized spinel $LiNi_xMn_{2-x}O_4$ (x = 0, 0.125, 0.25, 0.375, 0.5) cathode materials have spherical or spherical like morphology with particle size of micrometers. The examination of the X-Ray Diffraction patterns confirms that all the peaks are very sharp, indicating a high crystallinity of the powders.

First order derivative of TGA curves reveals the temperature at which the maximum decrease of mass occurs. The mass loss curve exhibited a continuous decrease of mass with temperature. The first cycle discharge capacity of pristine $LiMn_2O_4$ and $LiNi_{0.125}Mn_{1.875}O_4$ samples did not vary significantly. The first cycle discharge capacity of $LiNi_{0.125}Mn_{1.875}O_4$ is comparable to that of the pristine $LiMn_2O_4$, just as the values of their lattice parameter are essentially the same. The larger the lattice parameter, the easier the Li ions can more freely, thereby increasing the discharge capacity. The variation in lattice parameter as a result of Ni doping greatly increased the cyclability of discharge capacity of the $LiMn_2O_4$ spinel. Compared with the pristine $LiMn_2O_4$ cathode material, the $LiNi_{0.125}Mn_{1.875}O_4$ composition did not improve the cyclability, whereas the other doped spinel compositions do retain their initial capacities for many cycles; for example, Nickel doped compositions $LiNi_{0.25}Mn_{1.75}O_4$, $LiNi_{0.375}Mn_{1.625}O_4$, and $LiNi_{0.5}Mn_{1.5}O_4$, respectively, retain 1.5, 1.6, and 1.3 times that of pristine $LiMn_2O_4$. In addition, the $LiNi_{0.375}Mn_{1.625}O_4$ sample exhibited the more stable discharge capacity than the other samples. For cycles 2 through 10 there is a gradual decrease of the battery voltage for each cycle. It can also be seen that the 3 V discharge capacity decreases slightly when applying a 1 C discharge current and dramatically when

going above that. At 4 C, the battery delivers approximately 50% of the theoretical capacity before it reaches a cell voltage of 3 V.

References

[1] M. Winter, R.J. Brodd, What are batteries, fuel cells, and supercapacitors? Chem. **Rev**. 104 , 4245-4270 (2004).

[2] A.S. Arico, P. Bruce, B. Scrosati, J. Tarascon, W. Van Schalkwijk, Nanostructured materials for advanced energy conversion and storage devices, Nature materials **4**, 366-377 (2005).

[3] C. Masquelier, L. Croguennec, Polyanionic (Phosphates, Silicates, Sulfates) Frameworks as Electrode Materials for Rechargeable Li (or Na) Batteries, Chem. **Rev**. (2013).

[4] T. Ohzuku, M. Kitagawa, T. Hirai, Electrochemistry of Manganese Dioxide in Lithium Nonaqueous Cell III. X-Ray Diffractional Study on the Reduction of Spinel-Related Manganese Dioxide, J. Electrochem. Soc. **137**, 769–775 (1990).

[5] R. Gummow, A. De Kock, M. Thackeray, Improved capacity retention in rechargeable 4 V lithium/lithium-manganese oxide (spinel) cells, Solid State Ionics 69, 59–67 (1994).

[6] D.H. Jang, Y.J. Shin, S.M. Oh, Dissolution of Spinel Oxides and Capacity Losses in 4 V $Li/Li_xMn_2O_4$ Cells, J. Electrochem. Soc. **143** , 2204–2211 (1996).

[7] Y. Xia, T. Sakai, T. Fujieda, X. Yang, X. Sun, Z. Ma, et al., Correlating Capacity Fading and Structural Changes in $Li_{1+y}Mn_{2-y}O_{4-x}$ Spinel Cathode Materials: A Systematic Study on the Effects of Li/Mn Ratio and Oxygen Deficiency , J.Electrochem. Soc. **148**, A723–A729 (2001).

[8] A.A. Pesaran, Battery thermal models for hybrid vehicle simulations, Journal of Power Sources, **vol**. **110**, pp. 377-382 (2002).

[9] R. Sabbah, R. Kizilel, J.R Selman, Active (air cooled) vs. passive (phase change material) thermal management of high power lithium-ion packs: Limitation of temperature rise and uniformity of temperature distribution, Journal of Power Sources, **vol**. **182**, pp. 630-638 (2008).

[10] X. Gu, X. Li, L. Xu, H. Xu, J. Yang, Y. Qian, Synthesis of Spinel $LiNi_xMn_{2-x}O_4$ (x= 0, 0. 1, 0. 16) and Their High Rate Charge-Discharge Performances, Int. J.Electrochem. Sci **7**, 2504–2512 (2012).

[11] Y. Idemoto, H. Narai, N. Koura, Crystal structure and cathode performance dependence on oxygen content of $LiMn_{1.5}Ni_{0.5}O_4$ as a cathode material for secondary lithium batteries, J. Power Sources **119** , 125–129 (2003).

[12] H. Wu, J. Tu, X. Chen, Y. Li, X. Zhao, G. Cao, Effects of Ni-ion doping on electrochemical characteristics of spinel $LiMn_2O_4$ powders prepared by a spray-drying method, Journal of Solid State Electrochemistry **11**, 173–176 (2007).

[13] S.T. Myung, S. Komaba, N. Kumagai, H. Yashiro, H.T. Chung, T.H. Cho,Nano-crystalline $LiNi_{0.5}Mn_{1.5}O_4$ synthesized by emulsion drying method, Electrochim. Acta **47**, 2543–2549 (2002).

[14] J.H. Kim, S.T. Myung, C. Yoon, S. Kang, Y.K. Sun, Comparative Study of $LiNi_{0.5}Mn_{1.5}O_{4-x}$ and $LiNi_{0.5}Mn_{1.5}O_4$ Cathodes Having Two Crystallo graphic Structures: Fd 3 m and P 4332, Chemistry of materials **16**, 906–914 (2004).

[15] B. Hwang, Y. Wu, M. Venkateswarlu, M. Cheng, R. Santhanam, Influence of synthesis conditions on electrochemical properties of high-voltage $Li_{1.02}Ni_{0.5}Mn_{1.5}O_4$ spinel cathode material, J. Power Sources **193**, 828–833 (2009).

[16] H.L. Zhu, Z.Y. Chen, S. Ji, V. Linkov, Influence of different morphologies on electrochemical performance of spinel $LiMn_2O_4$, Solid State Ionics **179**, 1788–1793 (2008).

[17] B. Hwang, R. Santhanam, D. Liu, Y. Tsai, Effect of Al-substitution on the stability of $LiMn_2O_4$ spinel, synthesized by citric acid sol–gel method, J. Power Sources **102**, 326–331 (2001).

[18] S.J. Clark, M.D. Segall, C.J. Pickard, P.J. Hasnip, M.I. Probert, K. Refson, et al., First principles methods using CASTEP, Zeitschrift für Kristallographie **220**, 567-570 (2005).

[19] Deng, D., M. G. Kim, J. Y. Lee, and J. Cho.Green energy storage materials: Nanostructured TiO_2 and Sn-based anodes for lithium-ion batteries.Energ. Environ. Sci. **2**:818–837 (2009).

[20] P Touzain, R.Y., Insertion compounds of graphite with improved performances and electrochemical applications of those compounds,US (1986).

[21] Ehrlich, G.M., Lithium-ion batteries. (2002).

[22] Shimadzu, Rechargeable Lithium-Ion Battery Evaluation (2005).

[23] Zhao L Z, Hu S J, Ru Q, et al. Effects of Graphite on Electrochemical Performance of Sn/C Composite Thin Film Anodes'. Power Sources, pp.481-484 (2008).

[24] A. N. Dye. Electrochemical Alloying of Lithium in Organic Electrolytes. Journal of the Electrochemical Society , pp. 1547-1549 (1971).

[25] Madhu, C., J. Garrett, and V. Manivannan, Synthesis and characterization of oxide cathode materials of thesystem(1-x-y)LiNiO₂·xLi₂MnO<sub>3</sub&gt, yLiC oO<sub>2</sub&gt. Ionics, **16(7)**: p. 591-602 (2010).

[26] Sun, Y., et al., The preparation and electrochemical performance of solid solutions $LiCoO_2$–Li_2MnO_3 as cathode materials for lithium ion batteries. Journal of Power Sources, **159(2)**: p. 1353-1359 (2006).

[27] Jiang, J., et al, Structure, Electrochemical Properties, and Thermal Stability Studies of Cathode Materials in the xLi[Mn[sub 1/2]Ni[sub 1/2]]O[sub 2][bold [center-dot]]yLiCoO[sub 2][bold [center-dot]]zLi[Li[sub 1/3]Mn[sub 2/3]]O[sub 2] Pseudoternary System (x + y + z =, 1). Journal of The Electrochemical Society,**152(9)**: p. A1879-A1889 (2005).

[28] Zhong, Q., et al., Synthesis and Electrochemistry of LiNi[sub x]Mn[sub 2 - x]O[sub 4]. Journal of The Electrochemical Society, 144(1): p. 205-213 (1997).

[29] Zhong, S.-w., et al., Characteristics and electrochemical performance of cathode material Co-coated LiNiO2 for Li-ion batteries. Transactions of Nonferrous Metals Society of China, 16(1): p. 137-141 (2006).

[30] Chen, R. and M.S. Whittingham, Cathodic Behavior of Alkali Manganese Oxides from Permanganate. Journal of The Electrochemical Society, 144(4): p. L64-L67 (1997).

[31] Armstrong, A.R. and P.G. Bruce, Synthesis of layered $LiMnO_2$ as an electrode for rechargeable lithium batteries. Nature, 381(6582): p. 499-500 (1996).

[32] Thackeray, M.M., Structural Considerations of Layered and Spinel Lithiated Oxides for Lithium Ion Batteries. Journal of The Electrochemical Society, 142(8): p. 2558-2563 (1995).

[33] Amatucci, G., et al., The elevated temperature performance of the $LiMn_2O_4$/C system: failure and solutions. Electrochimica Acta, 45(1–2): p. 255-271 (1999).

[34] Shao-Horn, Y. and R.L. Middaugh, Redox reactions of cobalt, aluminum and titanium substituted lithium manganese spinel compounds in lithium cells. Solid State Ionics, 139(1–2): p. 13-25 (2001).

[35] Gummow, R.J., A. de Kock, and M.M. Thackeray, Improved capacity retention in rechargeable 4 V lithium/lithium-manganese oxide (spinel) cells. Solid State Ionics, 69(1): p. 59-67 (1994).

[36] Krins, N., et al., LiMn2−xTixO4 spinel-type compounds (x ≤ 1): Structural, electrical and magnetic properties. Solid State Ionics, 177(11–12): p. 1033-1040 (2006).

[37] Makimura, Y. and T. Ohzuku, Lithium insertion material of LiNi1/2Mn1/2O2 for advanced lithium-ion batteries. Journal of Power Sources, 119–121(0): p. 156-160 (2003).

[38] Ohzuku, T. and Y. Makimura, Layered Lithium Insertion Material of $LiNi_{1/2}Mn_{1/2}O_2$: A Possible Alternative to $LiCoO_2$ for Advanced Lithium-Ion Batteries. Chemistry Letters, 30(8): p. 744-745 (2001).

[39] Rossen, E., C.D.W. Jones, and J.R. Dahn, Structure and electrochemistry of $Li_xMn_yNi_{1-y}O_2$. Solid State Ionics, 57(3–4): p. 311-318 (1992).

[40] Spahr, M.E., et al., Characterization of Layered Lithium Nickel Manganese Oxides Synthesized by a Novel Oxidative Coprecipitation Method and Their Electrochemical Performance as Lithium Insertion Electrode Materials, Journal of The Electrochemical Society, 145(4): p. 1113-1121(1998).

[41] Yang, X.-Q., et al., Crystal structure changes of $LiMn_{0.5}Ni_{0.5}O_2$ cathode materials during charge and discharge studied by synchrotron based in situ XRD. Electrochemistry Communications, 4(8): p. 649-654 (2002).

[42] Lu, Z., D.D. MacNeil, and J.R. Dahn, Layered Cathode Materials Li[Ni[sub x]Li[sub (1/3 - 2x/3)]Mn[sub (2/3 - x/3)]]O[sub 2] for Lithium-Ion Batteries. Electrochemical and Solid-State Letters, 4(11): p. A191-A194 (2001).

[43] Neudecker, B.J., et al., Lithium Manganese Nickel Oxides Li[sub x](Mn[sub y]Ni[sub 1 - y])[sub 2 -x]O[sub 2]. Journal of The Electrochemical Society, 145(12): p. 4148-4159(1998).

[44] Ohzuku, T., et al., A 3-Volt Lithium-Ion Cell with $Li[N_{i1/2}Mn_{3/2}]O_4$ and $Li[Li1/3Ti_{5/3}]O_4$: A Method to Prepare Stable Positive-Electrode Material of Highly Crystallized $Li[Ni_{1/2}Mn_{3/2}]O_4$. Chemistry Letters, 30(12): p. 1270-1271 (2001).

[45] Kim, J.-S., et al., Electrochemical and Structural Properties of $xLi2M'O3\cdot(1-x)LiMn_{0.5}Ni_{0.5}O_2$ Electrodes for Lithium Batteries (M' = Ti, Mn, Zr; $0 \le x \leqslant 0.3$). Chemistry of Materials, 16(10): p. 1996-2006 (2004).

[46] Deng, D., M. G. Kim, J. Y. Lee, and J. Cho. Green energy storage materials: Nanostructured TiO_2 and Sn-based anodes for lithium-ion batteries.Energ. Environ. Sci. 2:818–837 (2009).

[47] Tarascon, J. M., and M. Armand. Issues and challenges facing rechargeable lithium batteries. Nature 414:359–367 (2001).

[48] Arico, A. S., P. Bruce, B. Scrosati, J. M. Tarascon, and W. Van Schalkwijk. Nanostructured materials for advanced energy conversion and storage devices.Nat. Mater. 4:366–377 (2005).

[49] Winter, M., J. O. Besenhard, M. E. Spahr, and P. Novak. Insertion electrode materials for rechargeable lithium batteries. Adv. Mater. 10:725–763 (1998).

[50] Poizot, P., S. Laruelle, S. Grugeon, L. Dupont, and J. M. Tarascon. Nano-sized transition-metaloxides as negative-electrode materials for lithium-ion batteries.Nature 407:496–499 (2000).

[51] Winter, M., and R. J. Brodd. What are batteries,fuel cells, and supercapacitors? Chem. **Rev**.104:4245–4269 (2004).

[52] S.T. Aruna, Combustion Synthesis Novel Routes to Novel Materials, Bentham Science Publishers 206–221 (2010).

[53] X. Yu, C. Zhou, X. He, Z. Peng, S. Yang, The influence of some processing conditions on luminescence of SrAl2O4: Eu2 nanoparticles produced by combustion method, Mater Lett **58** , 1087–1091 (2004).

[54] R. Santhanam, B. Rambabu, Research progress in high voltage spinel LiNi0.5Mn1.5O4 material, J. Power Sources **195**, 5442–5451 (2010).

[55] P. Hohenberg, W. Kohn, Phys. **Rev**. **136**, B864 (1964).

[56] J.P. Perdew, Y. Wang, Phys. **Rev**. B 45, 13244 (1992).

[57] J.P. Perdew, J. Chevary, S. Vosko, K.A. Jackson, M.R. Pederson,D. Singh, C. Fiolhais, Phys. **Rev**. B 46, 6671 (1992).

[58] D. Vanderbilt, Phys. **Rev**. B 41, 7892 (1990).

[59] H.J. Monkhorst, J.D. Pack, Phys. **Rev**. B 13, 5188 (1976).

[60] T.H. Fischer, J. Almlof, J. Phys. Chem. 96, 9768 (1992).

[61] M.A. Kebede, M.J. Phasha, N. Kunjuzwa, L.J. le Roux, D.Mkhonto, K.I. Ozoemena, M.K. Mathe, Sustain. Energy Technol.Assess. 5, 44 (2014).

[62] T. Kakuda, K. Uematsu, K. Toda, M. Sato, J. Power Sources **167**,499 (2007).